Rev. Roum. Sci. Techn.– Électrotechn. et Énerg.
Vol. **67**, *2*, pp. 181–185, Bucarest, 2022

A NOVEL DEAD-TIME ELIMINATION STRATEGY FOR VOLTAGE SOURCE INVERTERS IN INDUCTION HEATING SYSTEMS THROUGH FRACTIONAL-ORDER CONTROLLERS

ARIJIT CHAKRABARTI[1], PRADIP KUMAR SADHU[2], PALASH PAL[3]

Keywords: Dead-time; Full bridge series resonant inverter; Fuzzy control; Fractional-order proportional integral derivative, Induction heating; Voltage source inverter; Zero voltage switching.

The voltage source inverter (VSI) based induction-heating systems consisting of full-bridge series resonant inverters use power switching devices such as the insulated-gate-bipolar-transistor (IGBT) to achieve zero current switching or zero voltage switching operation. Such a configuration is susceptible to shoot-through during switching periods and avoidance of shoot-through is achieved through the introduction of the dead time in general. However, it necessitates the inclusion of dead-time compensators to eliminate the adverse effects of the dead time. This paper proposes a novel voltage source inverter dead-time compensation strategy for induction heating systems that uses the fractional order proportional integral derivative (FOPID) controller. Although the integer-order proportional integral derivative (IOPID) controller is widely used for induction heating systems, it does not remove the impact of dead time and does not act as a compensator. The study covers the design and optimal tuning of the fractional order PID controller for the VSI fitted induction-heating system using fuzzy logic and compares the performance of the fuzzy FOPID controller with the standard IOPID controller. The simulations and corresponding results confirm that the fuzzy FOPID controller can appropriately compensate for the dead-time impact and can be considered a suitable control strategy for such induction heating systems. Modeling and simulations have been performed using MATLAB/ SIMULINK.

1. INTRODUCTION

Induction heating has appeared as the favorite heating technique for industrial, medical, and domestic applications [1]. Typical induction heating systems consist of half-bridge or full-bridge series resonant voltage source inverters. Each leg of the inverter contains a couple of power switching devices like the insulated-gate-bipolar-transistor (IGBT) so that zero current switching (ZCS) or zero voltage switching (ZVS) operation is established. These IGBTs are assumed ideal. The two pulses responsible for turning them on and off and that are sent to the upper and lower IGBTs of each arm are supposed to be complementary. Switching on and off the two switches simultaneously is possible only in an ideal scenario. In practice, however, simultaneous switching on and off will result in a shoot-through in the voltage source inverter. To avoid the bridge shoot-through, the dead time is introduced in the system such that one IGBT is turned off first and the other turned on after the dead time is elapsed, thereby avoiding the bridge shoot-through caused by the asymmetrical turn-on and turn-off time of the IGBTs. Nevertheless, this dead time will lead to output waveform distortion, and voltage loss and will introduce harmonic distortions and nonlinearities in the system [19,20]. It can result in thermal runaway as well. Consequently, failure of IGBTs and the entire inverter is also a possibility [2,3].

To reduce the dead-time effects, most of the available solutions concentrate on dead-time compensation through complex compensators and expensive hardware [4–8]. In addition, the VSI-based induction heating system necessitates developing intelligent control strategies with high switching frequencies through soft-switching such as zero current switching (ZCS) or zero voltage switching (ZVS) [9–12]. Integer Order Proportional-Integral-Derivative (IOPID) controllers are extensively used in induction heating (IH) systems for controlling the output power of the inverters.

Thus, the problem here is twofold, *viz.*, establishing a proper control strategy to control the induction heating system output and eliminating the dead-time effects. For the first one, the use of an IOPID controller would have been a solution had there not been a dead time in the system, because an IOPID controller leads to poor control in presence of dead time. In general, dead-time problems are addressed through the implementation of dead-time compensators. The authors have tried to address the problem without implementing any standard dead-time compensator circuit, rather with the fuzzy FOPID controller, which improves the overshoot and minimizes the cost functions, giving another choice of dead-time elimination strategy implementation.

To resolve the dead-time problem, the authors have proposed a novel approach, which will eliminate the dead-time effects and concurrently control the system. Through the novel approach or strategy, a fractional order PID controller has been used for the first time to compensate for the dead time in the system. The fractional-order PID controller has been tuned using Fuzzy logic. The Fuzzy fractional order PID controller has been analyzed here for obtaining an improved and efficient closed-loop performance for power control of the induction heating system and to eliminate the dead time.

Although some research work has been done on fuzzy FOPID controllers for various systems, there is no research on fuzzy FOPID controllers for induction heating systems or as the dead-time compensator, and the feasibility and performance of fuzzy FOPID controllers with induction heating systems have not been explored much. Therefore, fuzzy FOPID has been selected as the intelligent control strategy for power control in induction heating systems and as the strategy to eliminate dead time in the system. Its performance has been compared with the IOPID controller,

[1]Department of Electrical Engineering, Indian Institute of Technology (ISM), Dhanbad, India, E-mail: a.chakra2010@gmail.com
[2]Department of Electrical Engineering, Indian Institute of Technology (ISM), Dhanbad, India, E-mail: pradip_sadhu@yahoo.co.in
[3]Department of Electrical Engineering, Haldia Institute of Technology, Haldia, West Bengal, India, E-mail: mail2palash@gmail.com

too. MATLAB/SIMULINK has been used to design and simulate here. The paper covers system modeling, design of the controllers, simulation, and results along with a conclusion at the end.

2. SYSTEM MODELLING

Figure 1 shows the typical arrangement of an induction heating (IH) system [12]. The uncontrolled rectifier rectifies the input ac voltage to generate direct current (dc) from alternating current (ac). The dc-link capacitor filters it and feeds it to the resonant inverter [12].

The inverter's high-frequency current generates an alternating magnetic field at the induction coil inducing eddy currents causing a hysteresis effect for heating up the workpiece. The load circuit comprising the workpiece and coil can be modeled like a transformer having single-turn secondary winding leading to the equivalent circuit consisting of a resistor R_{eqv} and an inductor L_{eqv}. A full-bridge series resonant inverter circuit is considered for the system here [17]. Figure 2 shows the full-bridge voltage source inverter topology.

The inverter includes four IGBTs as controllable switches (S_1 to S_4) with ultrafast anti-parallel soft recovery diodes (D_1 to D_4) and a series resonant circuit load having the equivalent resonant capacitance (C_{eqv}), resistance (R_{eqv}) and inductance (L_{eqv}). It is fed by a voltage source V. The switches operate at a higher switching frequency having switching period T_s. The series resonant circuit acts as the inductive load here.

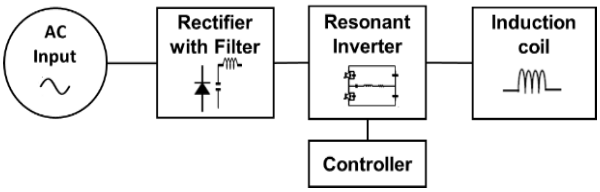

Fig. 1 – Typical induction heating system.

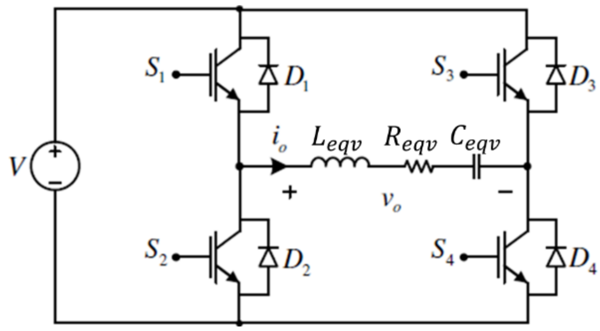

Fig. 2 – IH system having full-bridge resonant inverter.

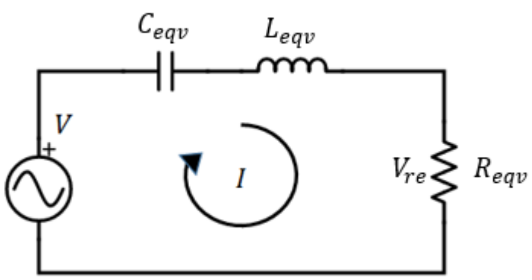

Fig. 3 – Simplified inverter circuit.

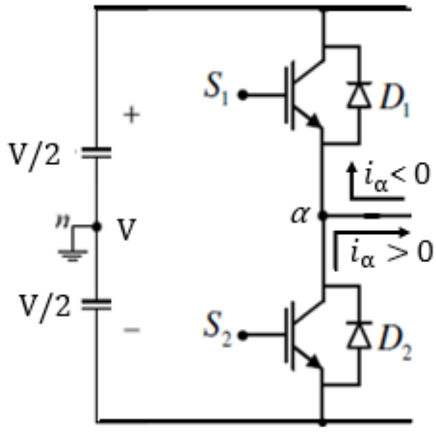

Fig. 4 – Typical VSI leg configuration.

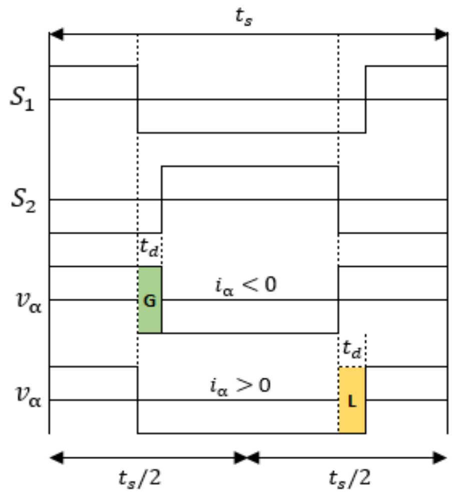

Fig. 5 – Switching patterns and output voltages including dead-time effect.

Figure 3 shows a simplified inverter circuit for calculating the transfer function of the voltage as it relates to the power that has got injected into the heating system straightway. Considering $V(s)$ as the input voltage, $V_{re}(s)$ the voltage across the equivalent resistance (R_{eqv}), ω the angular frequency, the voltage transfer function can be expressed by (1).

$$\frac{V_{re}(s)}{V(s)} = \frac{sR_{eqv}/L_{eqv}}{\left((s+\alpha)^2+\omega^2\right)} \tag{1}$$

where $\alpha = \dfrac{R_{eqv}}{2L_{eqv}}$ and $j\omega = \sqrt{\left(\dfrac{R_{eqv}}{2L_{eqv}}\right)^2 - \dfrac{1}{L_{eqv}C_{eqv}}}$.

The power across the load will be the response to the step $u(s) = 1/s$ and can be expressed as (2) [17].

$$W(s) = V_i^2 \frac{\beta_{re1}^{\;2}}{2R_{eqv}} \times \\ \times \frac{\left(\beta_{re2}^{\;2} - 2\beta_{re2} + 1\right)s^2 + \left(3 - 4\beta_{re2} + \beta_{re2}^{\;2}\right)\alpha s + 2\alpha^2}{s^3 + 3\alpha s^2 + 2\alpha^2 s}, \tag{2}$$

where V_i is the source peak voltage, $\beta_{re1} = \dfrac{2\left(\alpha + 2\omega^2\right)}{\left(\alpha^2 + 4\omega^2\right)}$, and $\beta_{re2} = \dfrac{\left(\alpha^2 + \alpha\omega + 2\omega^2\right)}{\left(\alpha + 2\omega^2\right)}$.

Now, the transfer function of the system is $P(s) = sW(s)$ and we finally get

$$P(s) = V_i^2 \frac{\beta_{re1}^{\ 2}}{2R_{eqv}} \times \\ \times \frac{\left(\beta_{re2}^{\ 2} - 2\beta_{re2} + 1\right)s^2 + \left(3 - 4\beta_{re2} + \beta_{re2}^{\ 2}\right)\alpha s + 2\alpha^2}{s^2 + 3\alpha s + 2\alpha^2}. \tag{3}$$

Referring to Fig. 2, we see that the inverter is a single-phase full-bridge series resonant two-level voltage source inverter. Figure 4 shows the typical VSI leg configuration. Figure 5 shows the switching patterns and output voltages for the dead-time effect. A dead time of t_d has been introduced in the VSI. The output voltage of this leg has been taken at point α. The inverter output voltage v_α will depend on the polarity of the current in each switching interval t_s. If the current is positive ($i_\alpha > 0$), the inverter output voltage v_α reduces signifying voltage loss (indicated by L in Fig. 5). Similarly, when the current is negative ($i_\alpha <$ 0), the inverter output voltage v_α increases signifying voltage gain (indicated by G in Fig. 5). While introducing the dead time, the delay in the system due to storage devices has also been considered and the overall dead time of 4μs has been considered for designing the controller so that the system remains stable over this range. This dead time will result in the transfer function is

$$P(s) = V_i^2 \frac{\beta_{re1}^{\ 2}}{2R_{eqv}} \times \\ \times \frac{\left(\beta_{re2}^{\ 2} - 2\beta_{re2} + 1\right)s^2 + \left(3 - 4\beta_{re2} + \beta_{re2}^{\ 2}\right)\alpha s + 2\alpha^2}{s^2 + 3\alpha s + 2\alpha^2} \times \\ \times e^{-0.4\times10^{-5}\,s}. \tag{4}$$

that provides information about the system required to design the control strategy including dead time in the system.

3. **CONTROLLER DESIGN**

3.1. INTEGER ORDER PID CONTROLLER

The integer order proportional-integral-derivative (IOPID) controller is the feedback controller that drives the induction heating system to be controlled by a weighted sum of the difference between output and target set point making the system less responsive to variations in the environment across and small variations in the system [13].

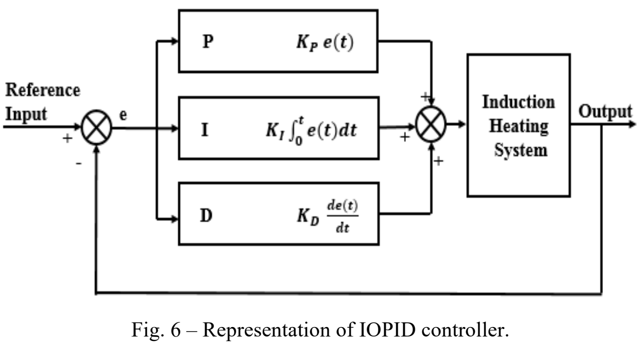

Fig. 6 – Representation of IOPID controller.

$$u_1(t) = \left[K_P e(t) + K_I \int_0^t e(t)dt + K_D \frac{de(t)}{dt} \right]. \tag{5}$$

Figure 6 shows an IOPID controller, the automatic choice for the process industry and it is utilized to enhance the dynamic response and minimize the steady-state error of the induction heating system. The Derivative controller will add a finite zero to the open-loop transfer function to enhance its transient response. The Integral controller will help reduce the steady-state error by adding a pole at the origin. The IOPID controller includes proportional, integral, and derivative controls with the output as expressed in (5).

Here K_P, K_I, and K_D are proportional, integral, and derivative gains. To design the IOPID controller, a set of K_P, K_I, and K_D is found through Ziegler-Nichols tuning, and the values have been considered as the initial values for tuning. MATLAB/SIMULINK PID tuning functionality has been leveraged to tune the IOPID controller and the parameters have been adjusted till a desired set of values is reached using the tool including the dead-time effect, which will improve the transient response of the system through the decrease in settling time and reduction in overshoot. The transfer function of the PID controller can be expressed as

$$C(s) = \left[K_P + \frac{K_I}{s} + sK_D \right]. \tag{6}$$

3.2. ADAPTIVE FUZZY FRACTIONAL ORDER PROPORTIONAL INTEGRAL DERIVATIVE CONTROLLER

The FOPID controller is the generalized IOPID controller [14–16]. It uses the generalized operator for integral and derivative definitions and is defined by (7).

$$u_c(t) = K_P e(t) + K_I D^{-\lambda} e(t) + K_D D^{\mu} e(t) \tag{7}$$

Here $u_c(t)$ is the controller output, $e(t)$ error signal; and K_P, K_I, and K_D the proportional, integral, and derivative gains of the controller. μ and λ the fractional power of differential and integral control[5]. For IOPID controller, λ = 1, μ = 1. Tuning of K_P, K_I, K_D, λ, and μ is achieved through fuzzy logic. Figure 7 shows the proposed adaptive fuzzy FOPID controller capable of tuning by itself. The tuner includes a fuzzification interface, the knowledge base, decision-making logic, and a defuzzification interface.

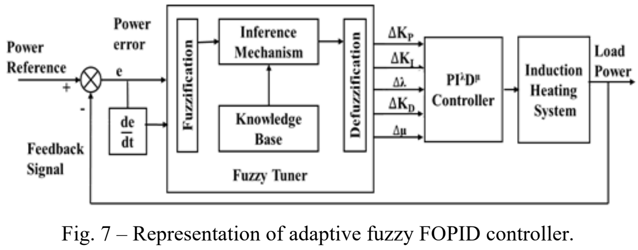

Fig. 7 – Representation of adaptive fuzzy FOPID controller.

The fuzzy controller model includes two input variables like error (e, the difference between output and reference set point) and rate of change of error (ce = de/dt), whereas five output variables (ΔK_P, ΔK_I, ΔK_D, $\Delta\lambda$, $\Delta\mu$) to tune the controller parameters K_P, K_I, K_D, λ, μ with respect the cost functions such as integral squared error (ISE), integral absolute error (IAE), integral time-weighted squared error (ITSE), integral time-weighted absolute error (ITAE) [17,18].

Figures 8a and 8b show membership functions for e and ce. Input variables have a universe of discourse divided into five overlapping fuzzy sets, *viz*., large negative (LN), medium negative (MN), zero error (ZE), medium positive (MP), and large positive (LP) while for output variables like small (S), medium-small (MS), medium (M), medium-large (ML) and large (L) as shown in Fig. 8c. The rule base has been built leveraging experience and knowledge comprising 25 IF-THEN rules with two antecedences and one consequence given by the fuzzy rule matrix mentioned in Table 1.

$$Rl_{\alpha,\beta,\gamma}\text{: IF } e=Al_{\alpha} \text{ AND } \Delta e=Bl_{\beta} \text{ THEN } u=Cl_{\gamma},$$

where $1 \le \alpha,\beta,\gamma \le 5$.

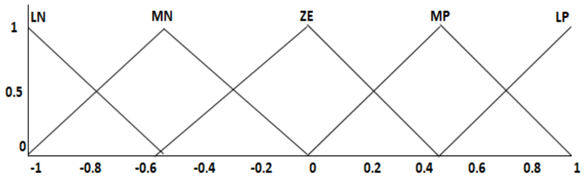

Fig. 8a – Membership functions for error (e).

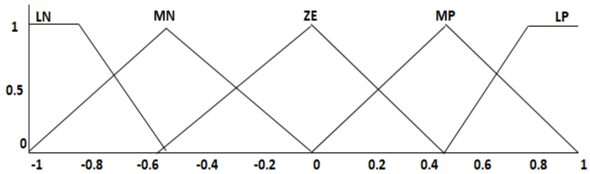

Fig. 8b – Membership functions for error change rate (ce).

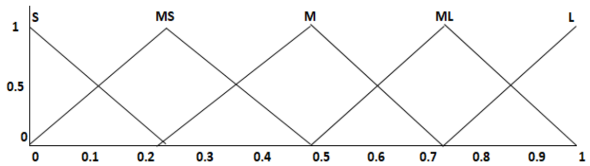

Fig. 8c – Membership functions for ΔK_P, ΔK_I, ΔK_D, $\Delta\lambda$, $\Delta\mu$.

Table 1

Fuzzy rule matrix

		ce				
		LN	*MN*	*ZE*	*MP*	*LP*
e	*LN*	*S*	*S*	*MS*	*MS*	*M*
	MN	*S*	*MS*	*MS*	*M*	*ML*
	ZE	*MS*	*MS*	*M*	*ML*	*ML*
	MP	*MS*	*M*	*ML*	*ML*	*L*
	LP	*M*	*ML*	*ML*	*L*	*L*

Table 2

Design specification and circuit parameters

Parameters	Values
Equivalent Resistance R_{eqv}	2.0 Ω
Equivalent inductance L_{eqv}	47.0 µH
Capacitance C_{eqv}	0.47 µF
Resonant Frequency f_r	33880 Hz
Switching Frequency f_s	35000 Hz
Inverter Input Voltage V	230 V

Table 3

Control parameters

Parameters	IOPID	FFOPID-ISE	FFOPID-IAE	FFOPID-ITSE	FFOPID-ITAE
K_P	3.0	$1.5\text{x}10^{-5}$	$1.1\text{x}10^{-5}$	$1.4\text{x}10^{-5}$	$1.2\text{x}10^{-5}$
K_I	2.4	$2.1\text{x}10^{-5}$	$2.2\text{x}10^{-5}$	$2.1\text{x}10^{-5}$	$2.3\text{x}10^{-5}$
K_D	$1.0\text{x}10^{-9}$	$1.5\text{x}10^{-7}$	$3.1\text{x}10^{-7}$	$2.0\text{x}10^{-7}$	$1.9\text{x}10^{-7}$
λ	1.0	0.9999	0.9998	0.9998	0.9998
µ	1.0	0.5237	0.4730	0.4979	0.5318

Table 4

Performance parameters

Controller	Overshoot %	Rise Time, s	Settling Time, s
IOPID	4.77	8.5×10^{-8}	3.0×10^{-4}
FFOPID-ISE	0.15	8.2×10^{-5}	1.4×10^{-2}
FFOPID-IAE	0.04	8.1×10^{-5}	5.2×10^{-3}
FFOPID-ITSE	0.89	1.3×10^{-3}	1.2×10^{-3}
FFOPID-ITAE	0.88	1.4×10^{-3}	1.3×10^{-3}

Table 5

Cost functions

Controller	ISE	IAE	ITSE	ITAE
IOPID	3.1×10^{-1}	5.8×10^{-1}	5.8×10^{-1}	5.8×10^{-1}
FFOPID-ISE	8.2×10^{-8}	-	-	-
FFOPID-IAE	-	9.9×10^{-8}	-	-
FFOPID-ITSE	-	-	2.4×10^{-8}	-
FFOPID-ITAE	-	-	-	4.9×10^{-8}

4. RESULTS AND DISCUSSION

Performances of the IOPID and self-tuning fuzzy FOPID (FFOPID) controllers have been simulated, analyzed, and compared for the IH system with the full-bridge series resonant inverter. Table 2 shows the circuit parameters. Table 3 gives the simulated controller parameters for IOPID and fuzzy FOPID parameters with optimization against various cost functions. Figure 9 provides step responses for a closed-loop IH system with IOPID control, while Fig. 10 provides step responses for fuzzy FOPID controllers with ISE, IAE, ITSE, and ITAE [12] as the cost functions, respectively.

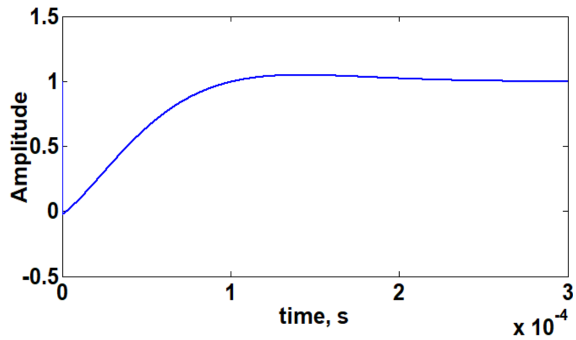

Fig. 9 – Step response of IH system having IOPID controller.

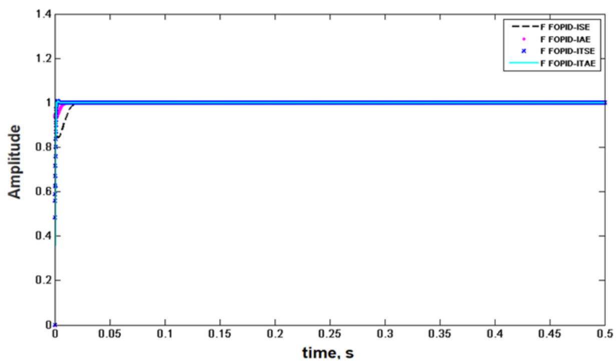

Fig. 10 – Step responses of IH system with fuzzy FOPID controller.

Overshoot, rise time, settling time, and values of ISE, IAE, ITSE, and ITAE for both the controllers are mentioned in Tables 4 and 5, respectively. The overshoot is 4.77 % for the IOPID controller, while less than 1 % for fuzzy FOPID controllers. The rise and settling times of the IOPID controller give better values though. The step responses also show smoothness and improved efficiency for the fuzzy FOPID controller. The proposed strategy of eliminating the effect of dead-time for VSI fitted induction heating system through fuzzy fractional order PID controller thus proves to be a suitable one and it successfully removes dead-time effects as well as controls the power output of the induction heating system efficiently.

5. CONCLUSION

To avoid the bridge shoot-through in voltage source inverters that use power-switching devices, dead time is added. But its inclusion in the system leads to various issues including voltage loss, output waveform distortion, nonlinearities, etc. This paper has proposed a novel dead-time elimination strategy for the voltage source inverters in induction heating systems using self-tuning fuzzy fractional-order PID controllers. The simulation results have shown that the induction heating system can more appropriately be controlled by such fuzzy fractional order PID controller, and it will eliminate the impact of dead time in the voltage source inverter within the induction heating system as well. The fuzziness of the controller yields improved robustness and control of the system. The systematic approach presented here can be applied to other systems that include voltage source inverter topologies.

Received on 12 August 2019.

REFERENCES

1. Ó. Lucía, P. Maussion, E.J. Dede, J.M. Burdío, *Induction heating technology, and its applications: past developments, current technology, and future challenges,* IEEE Transactions on Industrial Electronics, **61**, *5*, pp. 2509–2520 (2014).
2. L. Chen, F.Z. Peng, *Dead-time elimination for voltage source inverters*, IEEE Transactions on Power Electronics, **23**, *2*, pp. 574–580 (2008).
3. Y. Yang, K. Zhou, H. Wang, F. Blaabjerg, *Analysis and mitigation of dead time harmonics in the single-phase full-bridge PWM converter with repetitive controllers*, IEEE Transactions on Industry Applications, **54**, *5*, pp. 5343–5354 (2018).
4. A. Cichowski, J. Nieznanski, *Self-tuning dead-time compensation method for voltage-source inverters*, IEEE Power Electronics Letters, **3**, *2*, pp. 72–75 (2005).
5. N. Urasaki, T. Senjyu, K. Uezato, T. Funabashi, *An adaptive dead-time compensation strategy for voltage source inverter fed motor drives*, IEEE Transactions on Power Electronics, **20**, *5*, pp. 1150–1160 (2005).
6. K. Zhou, Y. Yang, F. Blaabjerg, D. Wang, *Optimal selective harmonic control for power harmonics mitigation*, IEEE Transactions on Industrial Electronics, **62**, *2*, pp. 1220– 1230 (2015).
7. T. Mannen, H. Fujita, *Dead time compensation method based on current ripple estimation*, IEEE Transactions on Power Electronics, **30**, *7*, pp. 4016–4024 (2015).
8. Y. H. Yang, K. Zhou, M. Cheng, *Phase compensation resonant controller for PWM converters*, IEEE Transactions on Industrial Informatics, **9**, *2*, pp. 957–964 (2013).
9. A. Chakraborty, D. Roy, T.K. Nag, P.K. Sadhu, N. Pal, *Open loop power control of a two-output induction heater*, Rev. Roum. Sci. Techn.– Électrotechn. et Énerg., **62**, *1*, pp. 48–54 (2017).
10. A. Chakraborty, P.K. Sadhu, A. Chakrabarti, A. Basak, N. Pal, *Asymmetrical duty cycle phase-shifted dual output induction cooker*, Rev. Roum. Sci. Techn.– Électrotechn. et Énerg., **63**, *1*, pp. 65–70 (2018).
11. A. Chakraborty, A. Chakrabarti, P.K. Sadhu, *Source current harmonics suppression in domestic induction heater*, Rev. Roum. Sci. Techn.– Électrotechn. et Énerg., **64**, *1*, pp. 45–50 (2019).
12. A. Chakrabarti, P. K. Sadhu, A. Chakraborty, P. Pal, *Brain Emotional Learning Based Intelligent Controller for Induction Heating Systems*, Rev. Roum. Sci. Techn.– Électrotechn. et Énerg., **63**, *1*, pp. 58–64 (2018).
13. P. K. Mohantya, B. K. Sahua, S. Pandab, *Tuning and assessment of proportional–integral–derivative controller for an automatic voltage regulator system employing local unimodal sampling algorithm*, Electric Power Components and Systems, **42**, *9*, pp. 959–969 (2014).
14. D. Vale´Rio, J. Sa` Da Costa, *Introduction to single-input, single-output fractional control*, IET Control Theory and Applications, **5**, *8*, pp. 1033–1057 (2011).
15. C.A. Monje, B.M. Vinagre, V. Feliu, Y.Q. Chen, *Tuning and auto-tuning of fractional order controllers for industry applications*, Control Engineering Practice, **16**, *7*, pp. 798–812 (2008).
16. C. Yeroglu, N. Tan, *Note on fractional-order proportional–integral–differential controller design*, IET Control Theory and Applications, **5**, *17*, pp. 1978–1989 (2011).
17. A. Chakrabarti, A. Chakraborty, P.K. Sadhu, *A fuzzy self-tuning PID controller with a derivative filter for power control in induction heating systems*, J. of Power Electronics, **17**, *6*, pp. 1577–1586 (2017).
18. X. Yang, C. Song, J. Sun, X. Wang, *Simulation and implementation of adaptive fuzzy PID*, Journal of Networks, **9**, *10*, pp. 2574–2581 (2014).
19. S. Furutani, A. Satake, T. Hozuki, *Inverter Dead Time Compensation Method using On-Line tuning*, IEEJ Journal of Industry Applications, **10**, *2*, pp. 264–272 (2020).
20. Y. Ji, Y. Yang, J. Zhou, H. Ding, X. Guo, S. Padmanaban, *Control strategies of mitigating deadtime effect on power converters: an overview*, Electronics (Switzerland), **8**, *2*, [196].